Supplemental Material for: Atomic-Scale Sliding Friction on Graphene in Water

J. G. Vilhena,[†,‖] Carlos Pimentel,[‡,⊥] Patricia Pedraz,[¶] Feng Luo,[¶] Pedro A. Serena,[†] Carlos M. Pina,[‡,⊥] Enrico Gnecco,[¶,#] and Rubén Pérez[*,§,@]

Instituto de Ciencia de Materiales de Madrid (ICMM), CSIC, c/ Sor Juana Ines de la Cruz 3, E-28049 Madrid, Spain, Departamento de Cristalografía y Mineralogía, Universidad Complutense de Madrid, E-28040 Madrid, Spain, Instituto Madrileño de Estudios Avanzados, IMDEA Nanociencia, Calle Faraday 9, E-28049 Madrid, Spain, and Departamento de Física Teórica de la Materia Condensada, Universidad Autónoma de Madrid, E-28049 Madrid, Spain

E-mail: ruben.perez@uam.es

[*]To whom correspondence should be addressed

[†]Instituto de Ciencia de Materiales de Madrid (ICMM), CSIC, c/ Sor Juana Ines de la Cruz 3, E-28049 Madrid, Spain

[‡]Departamento de Cristalografía y Mineralogía, Universidad Complutense de Madrid, E-28040 Madrid, Spain

[¶]Instituto Madrileño de Estudios Avanzados, IMDEA Nanociencia, Calle Faraday 9, E-28049 Madrid, Spain

[§]Departamento de Física Teórica de la Materia Condensada, Universidad Autónoma de Madrid, E-28049 Madrid, Spain

[‖]Departamento de Física Teórica de la Materia Condensada, Universidad Autónoma de Madrid, E-28049 Madrid, Spain

[⊥]Instituto de Geociencias (CSIC, UCM), E-28040 Madrid, Spain

[#]Otto Schott Institute of Materials Research, Friedrich Schiller University Jena, D-07742 Jena, Germany

[@]Condensed Matter Physics Center (IFIMAC), Universidad Autónoma de Madrid, E-28049 Madrid, Spain

1 Experiments

1.1 Friction measurements on G/Cu at different loads.

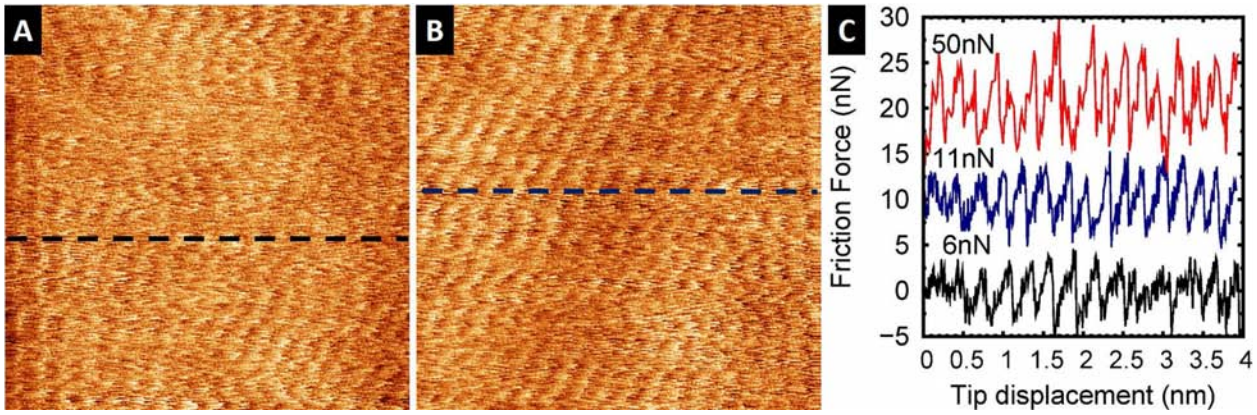

Figure S1: **(A)** High-resolution lateral force map (4×4 nm^2) on Gr/Cu. Normal load $F_N = 6$ nN. **(B)** Same as **(A)** for $F_N = 11$ nN. **(C)** Friction force cross-section at different loads corresponding to forward scans along the lines in **(A)**, **(B)**, and Fig. 1(B) in the paper ($F_N = 50$ nN).

2 MD Simulations for Friction

2.1 Simulation Protocol

Our simulation protocol starts placing the tip 1 nm away from the surface, followed by the system solvation, and a total energy minimization in order to avoid steric clashes. Thereafter, we stabilize the pressure (1 atm) and temperature (300 K), by letting the system to evolve for a period of 1 ns in a NPT ensemble. Once temperature and pressure are stabilized, we let the system evolve for a period of 10 ns in a NVT ensemble thus ensuring that atomic positions and velocities at the end of this period correspond to actual equilibrium configurations. Then, we indent the graphene surface with the diamond tip using constant velocity (0.1 m/s) Steered MD (SMD), as represented in the first row of Fig. S2. This allows us to obtain the atomic configurations that correspond to different indentation loads. Using these configurations, we resort again to constant velocity SMD (0.1 m/s) in order to scan the surface while measuring

the friction, as represented in the second row of figure S2. Note that both in the indentation and scanning protocol, the compliance of the cantilever and the upper body of the tip was modeled by coupling harmonic springs to the top layer of the tip. We have used kz = 100 N/m for the indentation and and kx,y = 10 N/m for the sliding, in accordance with previous works.[1,2]

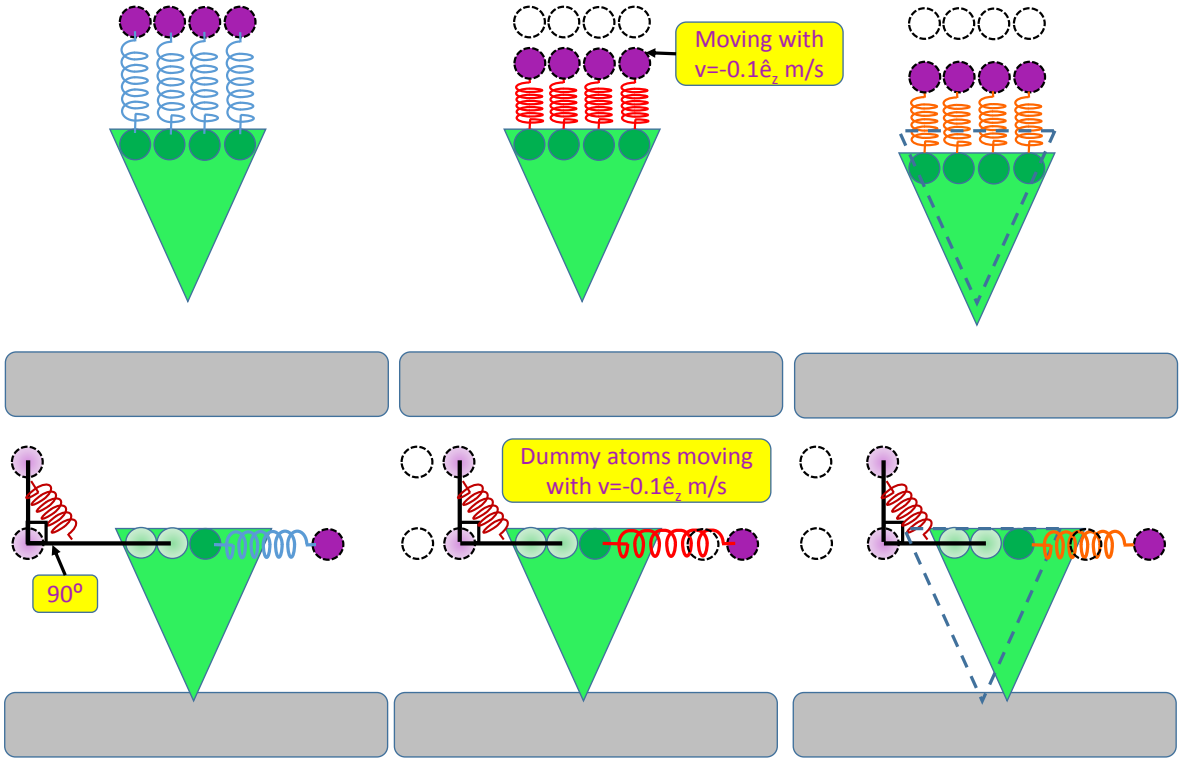

Figure S2: Schematic representation of the Steered-Molecular-Dynamics (SMD) protocols. In the first row we show a schematic representation of the SMD protocol used to obtain the indentation force curve shown in Fig. S3. In the second row we show a schematic representation of the SMD protocol used to scan the surface in order to measure the friction forces shown in the Fig. 2 of the manuscript. We represent the graphene in light-gray and the tip in light-green. The topmost atoms of the tip are represented in dark-green. In purple we represent the dummy-atoms, *i.e.* non-interacting, used to perform the SMD runs. The gradient colored atoms in the second row, assist the SMD-friction scan measurement maintaining the applied normal force constant as we scan the surface and also to avoid any twist of the tip occurring due to the friction with the surface. The springs represented in the first row images represent the k_z= 100 N/m, while the spring parallel to the surface represented in the second row images represent the kx,y = 10 N/m for the sliding.

2.2 Evaluating Friction forces from SMD simulations

Friction is any process by which mechanical energy is converted into thermal energy, *i.e.* conversion of work into heat. Therefore, by definition, friction is an irreversible process. A standard approach used to evaluate the free energy difference between two states A and B that do not need to obey the principle of microscopic reversibility is the Jarzynski equation (JE). The JE states that[3]

$$\begin{aligned} \exp\left\{\frac{-\Delta G_{AB}}{k_B T}\right\} &= \left\langle \exp\left\{\frac{-W_{A\to B}}{k_B T}\right\}\right\rangle_A \\ &= \frac{1}{N}\left(\exp\left\{\frac{-W^1_{A\to B}}{k_B T}\right\} + \exp\left\{\frac{-W^2_{A\to B}}{k_B T}\right\} + \ldots + \exp\left\{\frac{-W^N_{A\to B}}{k_B T}\right\}\right) , \end{aligned} \tag{1}$$

where k_B is the Boltzman constant, T is the temperature of the heat bath, ΔG_{AB} is the free energy difference between the initial (A) and final (B) state, $W_{A\to B}$ is the work required to take the system from A to B and $\langle . \rangle_A$ is the average over repeated (N) realizations of an external process that takes the system from (N) equilibrium configurations of the system in the state A to a new state B.

One of the most commonly used methods to take a system from state A to state B is steered molecular dynamics (SMD). SMD applies and external harmonic force onto a physical system thus driving the change in coordinates within certain time. This method should be thought as an umbrella sampling where the center of the restrain is time-dependent, as follows:

$$V_{ext} = \frac{1}{2}k[x - x_0(t)]^2 , \tag{2}$$

where x is the reaction coordinate (*e.g.* tip position on the surface), k is an elastic constant (usually chosen to match the cantilever compliance and lateral contact stiffness in FFM simulations[4]) and $x_0(t)$ is the reference position that is changing during the simulation in order to lead the change from state A to B. From this potential, we can extract a force in real time during our SMD. Furthermore by keeping a record of the actual displacement, we

can get the work performed *via*the SMD.

Table S1: Comparison of single SMD work values with the Jarzynski-free energy difference derived from these multiple SMD runs. All energies are in nN×Å. W_{AB} represents the work it takes to move the tip from position x=0.56 Å (position A) to x=0.76 Å (position B) obtained in 10 different SMD runs performed at a normal load of 20nN in a water environment (see Fig. 2C). Using these work values and the Jarzynski equality, we computed ΔG_{AB}, the free energy difference between A and B . Comparing this free energy with each independent SMD $W_{A\to B}$, the average energy difference is 3.7% with a maximum difference of 8.5%. Therefore, in this 0.2 Å displacement bin, the maximum deviation of each SMD force curve from the Jarzynski-free-energy derived force is 0.0035/(0.76-0.56)=0.0175 nN. Taking into consideration that we are measuring lateral force variations on the order of 1.2 nN, the difference between the free energy computed force and the force calculated from a single MD is negligible. Based on this test, we conclude that the SMD work values ($W_{A\to B}$) are a very good approximation free energy differences (ΔG_{AB}), thus correctly including the entropic contributions associated with the friction process. Note that each SMD run started 100 ps apart, thus guaranteeing that the initial configurations, while having the same reaction coordinate (x=0.56) were force uncorrelated (the stress tensor had already decayed and, thus, these starting configurations are not related in their initial forces).

(nN×Å)	run 1	run 2	run 3	run 4	run 5	run 6	run 7	run 8	run 9	run 10
W_{AB}	0.0430	0.0395	0.0433	0.0410	0.0430	0.0375	0.0421	0.0388	0.0415	0.0410
$\lvert W_{AB} - \Delta G_{AB}\rvert$	0.0020	0.0015	0.0023	0.0000	0.0020	0.0035	0.0011	0.0022	0.0005	0.0000
$\Delta G_{AB} = 0.0410$ nN×Å										

In general, a single SMD work curve cannot be taken as a free energy curve. Nevertheless, this approximation has been the workhorse of most of the nanoasperity friction works[4–9] performed in vacuum, and it gives results in very good agreement with the experiments,[5,6] In a water environment, we expect this approximation, *i.e.* $W_{A\to B} \approx \Delta G_{AB}$, to be valid, as long as we use slow enough tip velocities to ensure that the whole system stays close to an equilibrium state during the process (in particular, to avoid spurious water dragging forces). In order to test this approach in water, we have performed 10 different SMD runs moving the tip from position $x = 0.56$ Å (position A) to $x = 0.76$ Å (position B) for one of the indentation loads ($F_N = 20$ nN) in a water environment (see Fig. 2C). We have computed the work for each of these SMD runs, and compared them with the difference in ΔG_{AB} calculated using the Jarzynski equation (see Table S1). Each SMD run started 100 ps apart, thus guaranteeing that the initial configurations, while having the same reaction coordinate

(x=0.56) were force uncorrelated (the stress tensor had already decayed and, thus, these starting configurations are not related in their initial forces).

The results in Table S1 show that for a small displacement of the tip over the surface ($\Delta x = 0.2$Å), the dispersion of the work performed in each independent SMD translates into a maximum deviation of the friction force of 0.0175 nN, which is negligible when compared with friction values we are measuring (1.2 nN). Therefore the work computed in each SMD run can be taken, as a good approximation, as a free energy curve thus correctly accounting for the entropic contributions associated with the friction process.

2.3 Indentation curve and hydration layers on graphene.

Fig. S3 displays the simulated force during indentation and the atomic configurations at four different normal loads. Three interaction regimes can be clearly identified in Fig. S3A: weakly-interacting (d>6.5 Å), attractive (6.5<d<3.4 Å), and repulsive (d>3.4 Å), for both vacuum and water indentation. Nevertheless, in the latter, superimposed to these regimes, one can clearly distinguish two peaks on the force curve. The distance between them, *i.e.* ∼3 Å, matches the distance between the two water hydration layers formed on graphene reported in previous experimental and theoretical works.[10,11] Furthermore, by inspecting the MD trajectory of the indentation in water, one can clearly identify that these peaks, followed by a sharp decline in force, occur when the tip breaks the two hydration layers formed over graphene in water (see below for a detailed account of the process).

Given that we are indenting with a tip, in order to compare the position of the first hydration layer with the ones reported in the literature,[10–12] we must first understand how to relate our force curve with those distances. The interaction between the different non-bonded components in our system, *i.e.* tip, surface and water, is described by Lennard-Jones potentials. In these potentials,[13–16] the oxigen-carbon interaction enters the repulsive regime when the distance is lower than σ_{CO} =3.2 Å. Therefore, our diamond-*carbon* tip starts repelling the first hydration layer sitting over graphene (G) when the distance between the

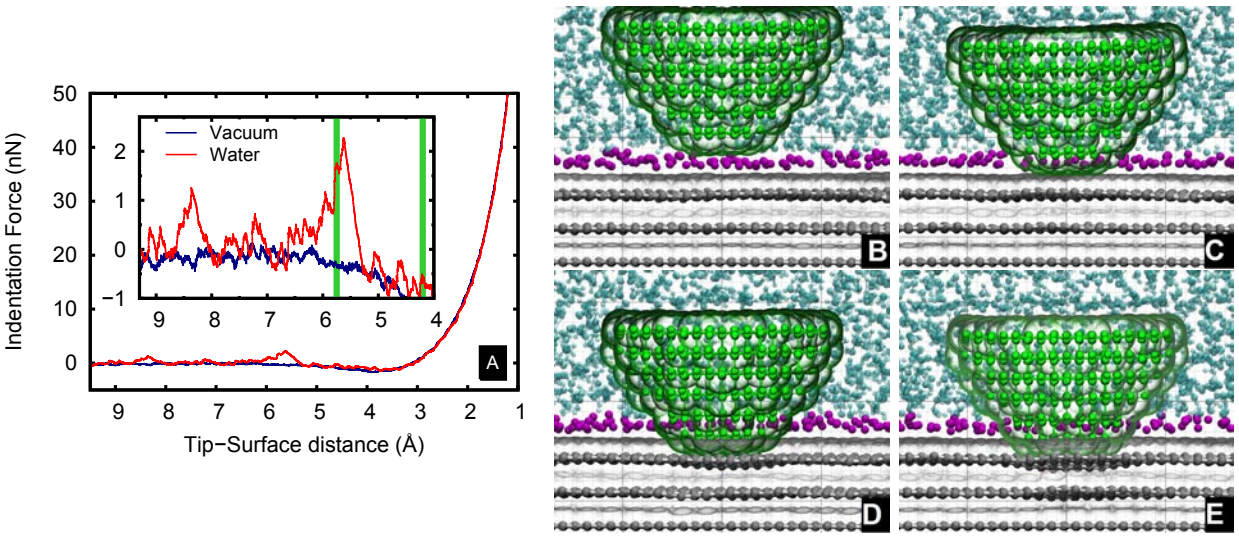

Figure S3: Forces and structures during indentation. The color code is the one used in Fig. 3 of the main manuscript. Besides the atomic configurations associated with the breaking of the first hydration layer (structures (B) and (C)), we also include the configurations at normal loads of 10 nN (D) and 20 nN (E).

tip and this layer is around σ_{CO} =3.2 Å. Inspecting the water force curve (Fig. S3A), we realize that the tip starts to feel an increasingly high repulsion when the tip-surface distance is d_{tip-G} =6.4 Å. Consequently, the first hydration layer is positioned at $d_{1^{st}wl-G}$ =d_{tip-G} − σ_{CO}=3.2 Å away from the graphene, which is, again, in excellent agreement with previously reported values .[10–12] Although this agreement could be anticipated, considering that the force fields we use are known to accurately reproduce graphene hydration properties,[13–16] its interesting to realize that our simulation protocol is sensitive enough to detect the presence of a weakly bounded hydration layer over graphene.

Fig. S4 illustrates the process of breaking the first hydration layer, *i.e.* displaying the simulation results for the tip-sample distance range between the two tip positions that corresponds to the two green lines shown in the inset of figure S3(A). In Fig. S4, carbon atoms and bonds in the diamond tip (top diameter = 2.2 nm; Contact diameter = 1.0 nm) are represented in green. The oxygen atoms of the water molecules in the first hydration layer are displayed in purple, while light gray is used for the carbon atoms in the three-layer graphene slab. (size = 5×5 nm^2). All the water molecules present on the system that are

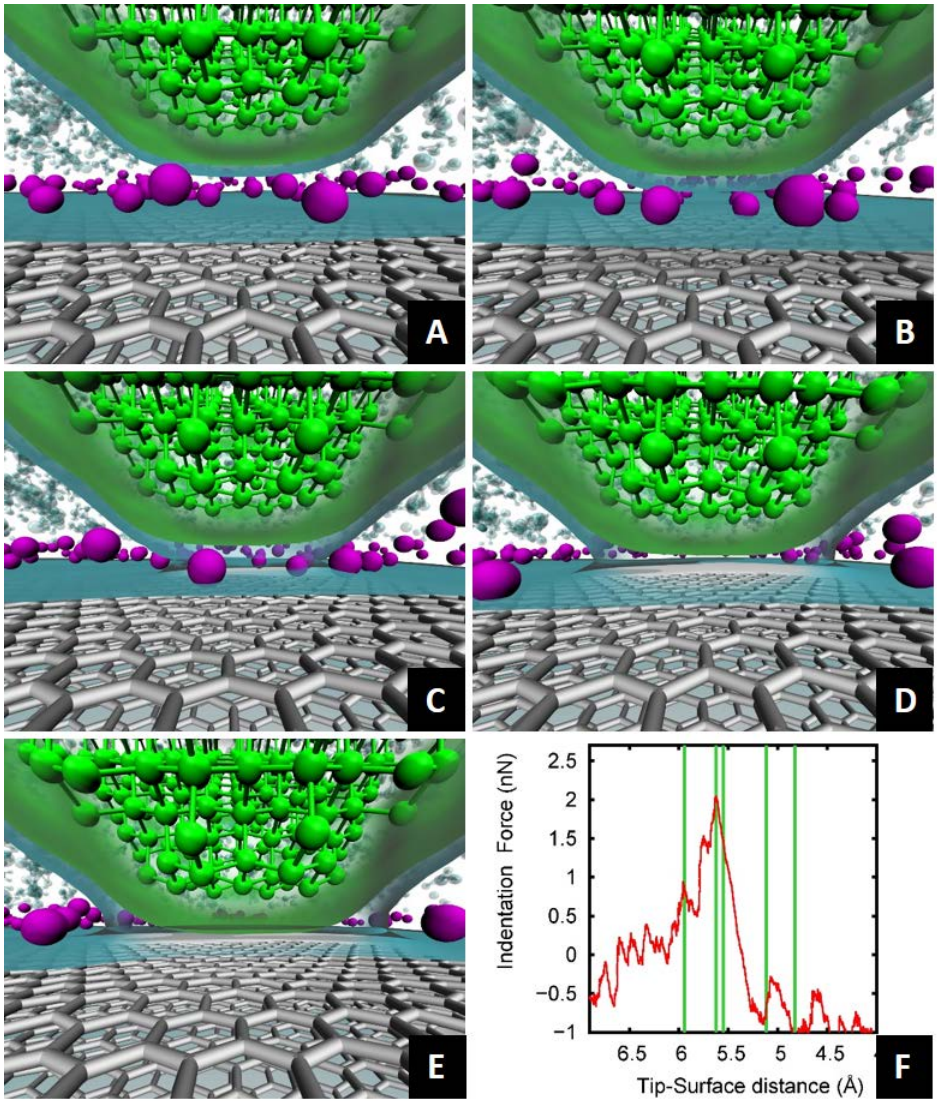

Figure S4: (A-E) Atomic configurations at different normal loads before (A,B) and after (C,D,E) breaking the first hydration layer (see text for details). (F): Zoom of the indentation curve shown in Fig. S3A around the force peak occurring due to the breaking of the first hydration layer. The green vertical lines in (F) correspond, from left to right, to the normal load and tip-surface distance of the configurations shown in (A), (B), (C), (D), (E), respectively.

directly above graphene and not in the first hydration layer are represented in transparent cyan. We have used a perspective view that allow us to see in greater detail the breaking of the hydration layer. In order to get insight into the breaking process, we also display the van der Waals (vdW) surfaces (*i.e.* σ_{CC}=3.4 Å) of graphene (gray) and the tip (green), and the solvent accessible surface area (SASA)[13] (transparent cyan surface) for the system composed by tip and surface.

In Fig. S4A, water molecules (purple) still have access to the tip-graphene gap, although a they are quickly bounced off the tip vdW surface (green), due to the repulsion imposed by the tip on the first hydration layer. The breaking of the first hydration layer, corresponding to a maximum in the indentation force, is marked by the union of the SASA from the tip and the surface (Fig. S4B). During the rest of the indentation, Figs.S4C-E, we observe the continuous growth of the the region between the tip and the surface where water molecules are excluded.

2.4 Rapid decay of the water stress memory.

Figure S5 illustrates how the water stress memory is lost in the slip phase, the fastest process during the tip sliding. Before the slip phase, 102 water molecules were within 4.4 Å of the tip (Figs. S5B,D). After the slip phase, only 5 out of these 102 water molecules remained within an interacting distance of the tip (Figs. S5C,E). The positions of the 5 molecules have changed and, at certain stages of the slip phase, they were out of the reach of the interaction with the tip. These results clearly show that the movement of the water molecules is much faster than the velocity at which the tip moves, and further confirm that the very different water/tip time scales ensure that the water interaction felt by the tip is a purely stochastic one.

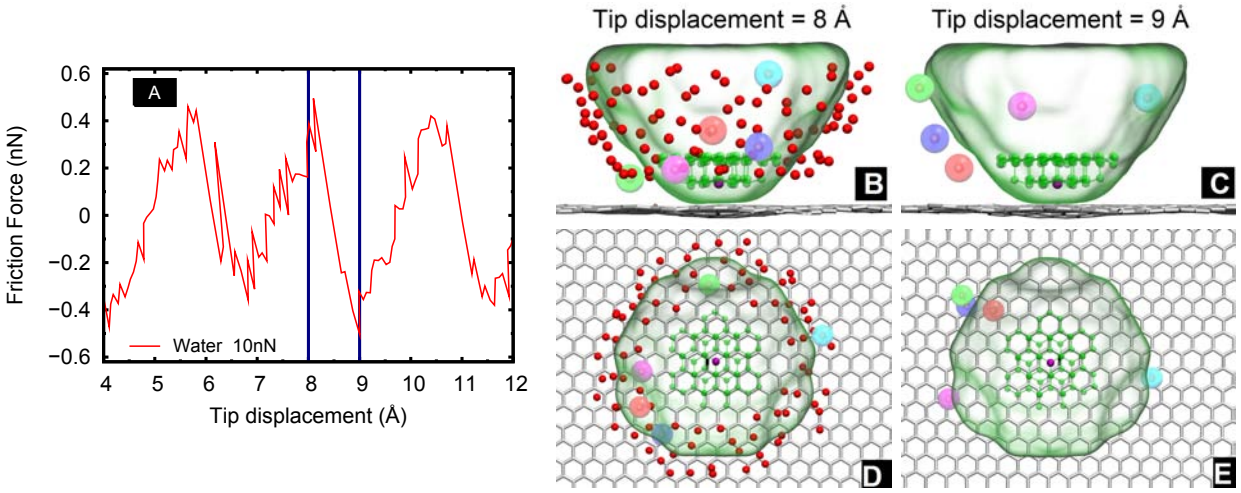

Figure S5: (A) Friction force measured in aqueous environment at a normal load of 10 nN. The blue lines indicate the times, right before and after the tip slip, at which the (B,D) and (C,E) images were taken. Lateral (B) and top (D) view of the water–oxygen atoms that are in contact with the tip just immediately before the slip. We display in red all the oxygen atoms that are within 4.4 Å of the tip at this stage. The large colored spheres represent the oxygen atoms that are still in contact with the tip after the slip phase (C,E). The green transparent surface corresponds to the van der Walls surface of the tip. The transparent green ball-stick-model atoms represent the tip atoms that are in contact with the surface, while the silver atomic layer corresponds to the top graphene layer in contact with the tip (the other two have been omitted).

References

1. Li, Q.; Dong, Y.; Perez, D.; Martini, A.; Carpick, R. W. Speed Dependence of Atomic Stick-Slip Friction in Optimally Matched Experiments and Molecular Dynamics Simulations. *Phys. Rev. Lett.* **2011**, *106*, 126101.

2. Dong, Y.; Wu, X.; Martini, A. Atomic Roughness Enhanced Friction on Hydrogenated Graphene. *Nanotechnology* **2013**, *24*, 375701.

3. Jarzynski, C. Nonequilibrium Equality for Free Energy Differences. *Phys. Rev. Lett.* **1997**, *78*, 2690–2693.

4. Dong, Y.; Li, Q.; Martini, A. Molecular Dynamics Simulation of Atomic Friction: A Review and Guide. *J. Vac. Sci. Tech. A* **2013**, *31*, –.

5. Li, Q.; Dong, Y.; Perez, D.; Martini, A.; Carpick, R. W. Speed Dependence of Atomic Stick-Slip Friction in Optimally Matched Experiments and Molecular Dynamics Simulations. *Phys. Rev. Lett.* **2011**, *106*, 126101.

6. Liu, X.-Z.; Ye, Z.; Dong, Y.; Egberts, P.; Carpick, R. W.; Martini, A. Dynamics of Atomic Stick-Slip Friction Examined with Atomic Force Microscopy and Atomistic Simulations at Overlapping Speeds. *Phys. Rev. Lett.* **2015**, *114*, 146102.

7. Li, Q.; Liu, X.-Z.; Kim, S.-P.; Shenoy, V. B.; Sheehan, P. E.; Robinson, J. T.; Carpick, R. W. Fluorination of Graphene Enhances Friction Due to Increased Corrugation. *Nano Lett.* **2014**, *14*, 5212–5217, PMID: 25072968.

8. Pugno, N.; Yin, Q.; Shi, X.; Capozza, R. A Generalization of The Coulombs Friction Law: From Graphene to Macroscale. *Meccanica* **2013**, *48*, 1845–1851.

9. Verhoeven, G. S.; Dienwiebel, M.; Frenken, J. W. M. Model Calculations of Superlubricity of Graphite. *Phys. Rev. B* **2004**, *70*, 165418.

10. Zhou, H.; Ganesh, P.; Presser, V.; Wander, M. C. F.; Fenter, P.; Kent, P. R. C.; Jiang, D. E.; Chialvo, A. a.; McDonough, J.; Shuford, K. L. *et al.* Understanding Controls on Interfacial Wetting at Epitaxial Graphene: Experiment and Theory. *Phys. Rev. B* **2012**, *85*, 035406.

11. Tocci, G.; Joly, L.; Michaelides, A. Friction of Water on Graphene and Hexagonal BN from Ab-Initio Methods : Very Different Slippage Despite Very Similar Interface Structures. *Nano Lett.* **2014**, *14*, 6872–6877.

12. Suzuki, K.; Oyabu, N.; Kobayashi, K.; Matsushige, K.; Yamada, H. Atomic-Resolution Imaging of Graphite-Water Interface by Frequency Modulation Atomic Force Microscopy. *Appl. Phys. Express* **2011**, *4*, 125102.

13. Wang, J. M.; Wolf, R. M.; Caldwell, J. W.; Kollman, P. A.; Case, D. A. Development and Testing of a General Amber Force Field. *J. Comput. Chem.* **2004**, *25*, 1157–1174.

14. Abascal, J. L.; Vega, C. A General Purpose Model for The Condensed Phases of Water: TIP4P/2005. *J. Chem. Phys.* **2005**, *123*, 234505.

15. Abascal, J. L. F.; Sanz, E.; Fernández, R. G.; Vega, C. A Potential Model for The Study of Ices and Amorphous Water: TIP4P/Ice. *J. Chem. Phys.* **2005**, *122*, 234511.

16. Vega, C.; Abascal, J. L. F.; Sanz, E.; MacDowell, L. G.; McBride, C. Can Simple Models Describe The Phase Diagram of Water? *J. Phys.: Condens. Matter* **2005**, *17*, S3283–S3288.